Journal of Molecular Graphics and Modelling 27 (2008) 131–139

Contents lists available at ScienceDirect

Journal of Molecular Graphics and Modelling

journal homepage: www.elsevier.com/locate/JMGM

Chemical function-based pharmacophore development for novel, selective kappa opioid receptor agonists

Nidhi Singh [a], Tammy L. Nolan [a], Christopher R. McCurdy [a,b,c,*]

[a] Department of Medicinal Chemistry and Laboratory for Applied Drug Design and Synthesis, The University of Mississippi, Mississippi 38677, USA
[b] Department of Pharmacology, The University of Mississippi, Mississippi 38677, USA
[c] Research Institute of Pharmaceutical Sciences, School of Pharmacy, The University of Mississippi, Mississippi 38677, USA

ARTICLE INFO

Article history:
Received 15 January 2008
Received in revised form 14 March 2008
Accepted 19 March 2008
Available online 28 March 2008

Keywords:
Kappa opioid receptor
Pharmacophore
Peripherally restricted
Agonist
Analgesics
New chemical entities (NCEs)
G-protein coupled receptor (GPCR)

ABSTRACT

In an effort to reduce or eliminate the centrally associated side effects produced by opioid analgesics there has been an interest in the preparation of peripherally acting opioid receptor agonists. These compounds would have very limited or no access to the central nervous system. As a first step towards developing peripheral kappa opioid receptor (KOP) agonists, we have developed a quantitatively predictive chemical function-based pharmacophore model of selective kappa opioid receptor agonists by using the HypoGen algorithm implemented in the Catalyst software. The input for HypoGen was a training set of 26 KOP agonists exhibiting K_i values ranging between 0.015 nM and 2300 nM. The best output hypothesis consists of four features: one hydrophobic (HYD), one ring aromatic (RA), one hydrogen bond acceptor (HBA), and one positive ionizable (PI) function. The predictive power of the model could be demonstrated by internal and external validation of the generated hypothesis. The resulting Catalyst pharmacophore can be used concurrently for rapid virtual screening of chemical databases to identify novel, selective KOP agonists that may be easily restricted to target tissues by synthetic modification. It is anticipated that such an approach will lead to the generation of novel selective KOP agonists that are clinically useful for the treatment of pain through peripheral mechanisms.

1. Introduction

The μ-, κ-, and δ- opioid G-protein coupled receptors, MOP, KOP, and DOP, respectively are the targets responsible for pharmacological effects exhibited by opioid-type drugs. All three appear to be present in the central and peripheral nervous system of many organisms including humans [1,2]. Although activation of all three receptor subtypes is known to produce antinociception, the majority of opioid drugs that are currently in clinical use as analgesic agents (e.g. morphine and fentanyl) are MOP agonists [3]. However, MOP stimulation is also responsible for the spectrum of unwanted side effects associated with opioids including respiratory depression, dependence liability, and inhibition of gastrointestinal motility [4]. It has been established by Martin et al. that KOP agonists are capable of producing analgesia without the side effects common to morphine and other classical opioids [5].

This led to considerable attention focused on the development of KOP agonists as potent and efficacious analgesics putatively devoid of the undesirable side effects seen with MOP analgesics. Although KOP agonists initially held great promise as analgesics, in due time, however, clinical studies with the centrally acting KOP agonists, spiradoline and enadoline revealed that these too were accompanied by their own set of central nervous system (CNS) liabilities, namely sedation and dysphoria [6,7]. These side effects prevented the continued clinical development and commercialization of KOP agonists as analgesics. With the identification of KOPs outside the CNS, it was hypothesized that peripheral KOP agonists could be developed to exhibit significant antinociceptive activity without their associated CNS side effects [8,9]. With this, there has been a renewed interest in the development of peripherally selective KOP agonists.

These peripherally acting analgesics exert effects via agonism of both peripherally located KOPs and possibly, for some non-peptidic KOP agonists, additional non-opioid molecular targets such as sodium channels located on primary sensory afferents. Peripheral opioid receptors are particularly important in inflammatory pain states and in the response to pruritogenic stimuli, and have also been implicated in the transmission of visceral pain.

* Corresponding author at: Department of Medicinal Chemistry, School of Pharmacy, The University of Mississippi, University, Mississippi 38677, USA.
Tel.: +1 662 915 5882; fax: +1 662 915 5638.
E-mail address: cmccurdy@olemiss.edu (C.R. McCurdy).

1093-3263/$ – see front matter © 2008 Elsevier Inc. All rights reserved.
doi:10.1016/j.jmgm.2008.03.007

Several studies have indicated the usefulness of such agonists in the treatment of pain conditions ranging from postoperative pain associated with abdominal surgery, intestinal, pancreatic and labor pains, dysmennorhea, and functional disorders such as irritable bowel syndrome (IBS) and dyspepsia [10].

New drug discovery programs are now initiated towards the design of peripherally selective KOP agonists. Several routes have been developed to obtain peripherally confined agents through modifications of centrally acting KOP agonists. Altering compound lipophilicity is a traditional approach used by medicinal chemists for reducing CNS penetration. This is often achieved by the incorporation of hydrophilic groups or designing charged or amphiphilic molecules. Attempts to synthesize zwitterionic analogs of the existing centrally acting KOP agonists have also been reported in literature [11]. An additional approach for restricting compounds to the periphery is the incorporation of elements that would render the compound a substrate for efflux pumps at the blood brain barrier, effectively pumping the compound out of the brain. Asimadoline (EMD 61753), the first peripherally selective KOP agonist to enter clinical trials, represents a proof of concept, thus the development of new potent, peripherally selective KOP agonists is well founded [12–17].

As a first step towards achieving this goal and in the absence of direct structural information of KOP, a systematic study was initiated to develop a pharmacophore hypothesis that may serve as a powerful search tool to be utilized as a 3D query for chemical databases to identify new chemical entities (NCEs) as potential KOP agonists. Additionally, the generated pharmacophore may also be used as a predictive tool for estimating biological activity of potential compounds based on structure–activity analyses.

2. Materials and methods

2.1. Molecular modeling

Molecular modeling was performed on a Silicon Graphics Octane2 R12000 dual processor workstation running on Irix 6.4 operating system (SGI, 1600 Amphitheater Parkway, Mountain View, CA 94043). Pharmacophore modeling was performed using *Catalyst 4.8* [18].

2.2. Biological data

The activity data for selective KOP agonists, represented as K_i in nM, were obtained from the literature [15–17,19–34]. The chemical structures of the agonists are listed in Figs. 1 and 2. The datasets were divided into a training set and a test set. For estimation (prediction) purposes, the activity values were classified based on a KOP agonistic activity scale: highly active ($\leq$1 nM, +++), moderately active ($1 < 100$ nM, ++), active ($100 \leq 500$ nM, +) and inactive (> 500 nM, −). This classification scheme is more consequential than actual prediction values, since one of the major uses of a pharmacophore model is its use in virtual screening of 3D chemical databases to identify lead compounds. The selection of a suitable training set is critical for the quality of automatically generated pharmacophore models [35]. To ensure the statistic relevance of the calculated model, the training set should contain a set of diverse compounds and their activity values. These should originate from comparable binding assays and spread equally over at least 4–5 orders of magnitude. Each selected compound should add some new information to the model while avoiding redundancy and bias both in terms of structural features and activity range. The most active compounds should be included so that they provide information on the most critical features required for a pharmacophore. On the basis of the above criteria, 26 compounds for the training set and 12 compounds for the test set were selected.

2.3. Generation of pharmacophores

A pharmacophore model in *Catalyst* is generally referred to as a 'hypothesis' which consists of a collection of features necessary for the biological activity of the ligands oriented in 3D space [36]. In order to generate a pharmacophore, all molecules (both training and test sets) were built and minimized within the *Catalyst* software. All stereoisomeric centers in the molecules were appropriately assigned as indicated in the original data sources. Conformation models for all of the molecules were generated using the quasi-exhaustive *Catalyst*/ConFirm module within the software, using the "best quality" conformational search option. A maximum of 250 conformations were generated using the CHARMm force field parameters and a constraint of 20 kcal/mol energy thresholds above the global energy minimum [37]. *Catalyst* selects conformers using the Poling algorithm, that penalizes any newly generated conformer that is too close to an already formed conformer in the set [38]. This method ensures maximum coverage in conformational space. All other parameters were set to the default settings.

An initial analysis of the "show function mapping" tools revealed that positive ionizable (PI), hydrogen bond acceptor (HBA), hydrophobic (HYD), and ring aromatic (RA) features could effectively map all the critical chemical/structural features of all the training set molecules. Therefore, these features were used to generate 10 pharmacophore hypotheses from the training set, using a default uncertainty value of 3. The uncertainty value represents a ratio range of uncertainty in the activity value based on the expected statistical irregularities of biological data collection. The *Catalyst*/HypoGen module can only generate a maximum of five features for a hypothesis. The best model was selected on the basis of a high correlation coefficient, lowest total cost, and rms values.

In general, HypoGen tries to construct a pharmacophore that gives the best correlation of the 3D arrangement of features with their corresponding pharmacological activities in a given set of training compounds. The resulting hypotheses are 3D arrangements of several default feature types (e.g. hydrogen bond acceptor, hydrogen bond donor, hydrophobic, ring aromatic, negative/positive ionizable) located at defined positions (location constraints). These are surrounded by certain spatial tolerance spheres, designating the area in space to be occupied by the corresponding chemical functions of the matched molecule. Each of the features is assigned a certain weight that is proportional to its relative contribution to the biological activity. Hydrogen bond acceptors/donors, and aromatic rings include an additional vector, defining the direction of the interaction.

The HypoGen algorithm ideally produces hypotheses that are common among the active compounds of the training set but do not reflect the inactive ones. The overall assumption is based on Occam's razor [39] which states that the simplest model is best between otherwise equivalent alternatives, thus constructing a model that correlates best with measured activities and that consists of as few features as possible. During a HypoGen run, three phases are passed through: (a) pharmacophores that best accommodate the most active compounds are elaborated in the constructive phase. (b) Those pharmacophores that fit the inactive training set members are abolished in the subtractive phase. (c) The remaining hypotheses are refined in the optimization phase. Moreover, the hypotheses are optimized by random translations of features, rotations of vectored

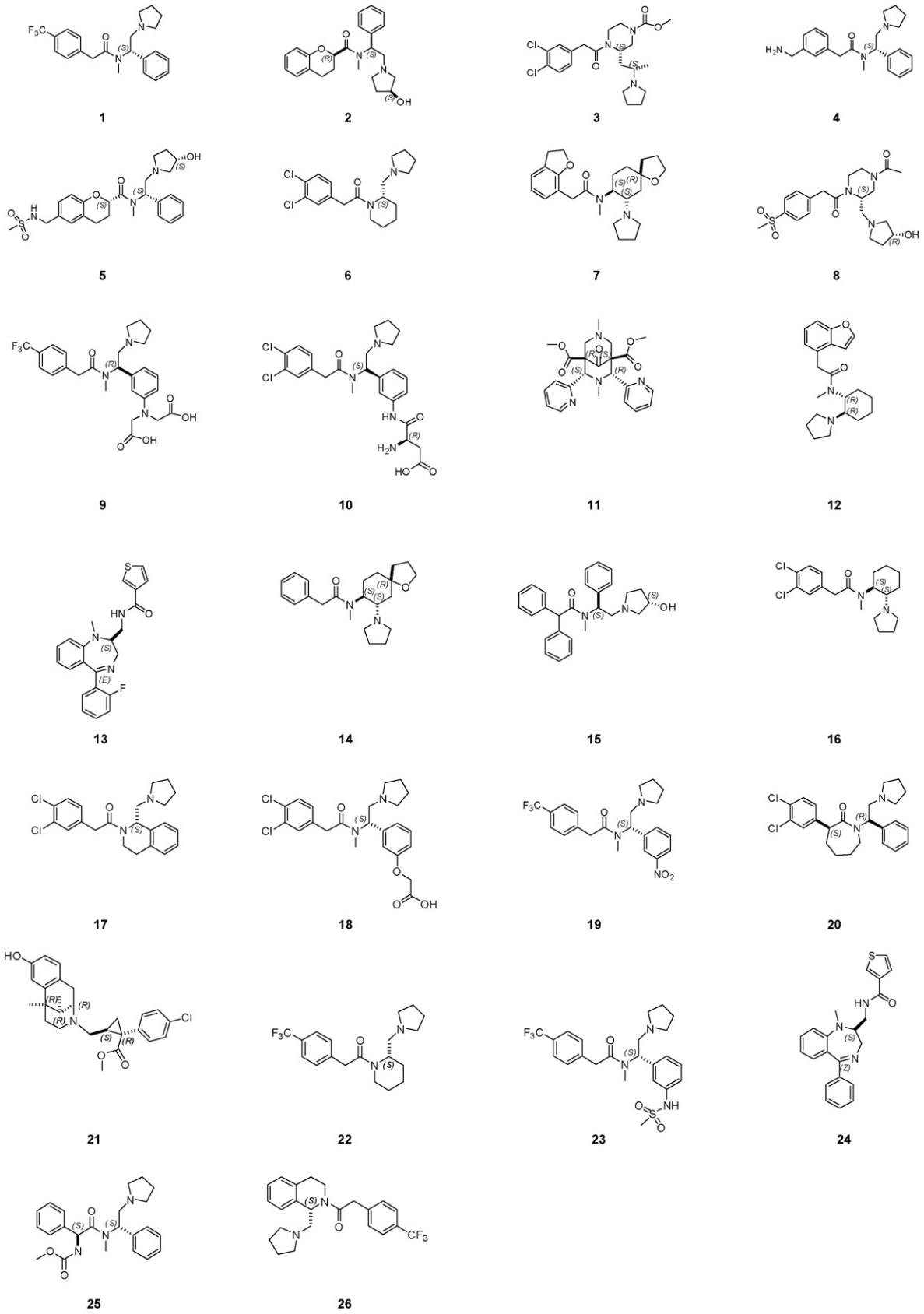

Fig. 1. Structures of compounds in training set. All structures were drawn using *ChemDraw Ultra* 8.0.

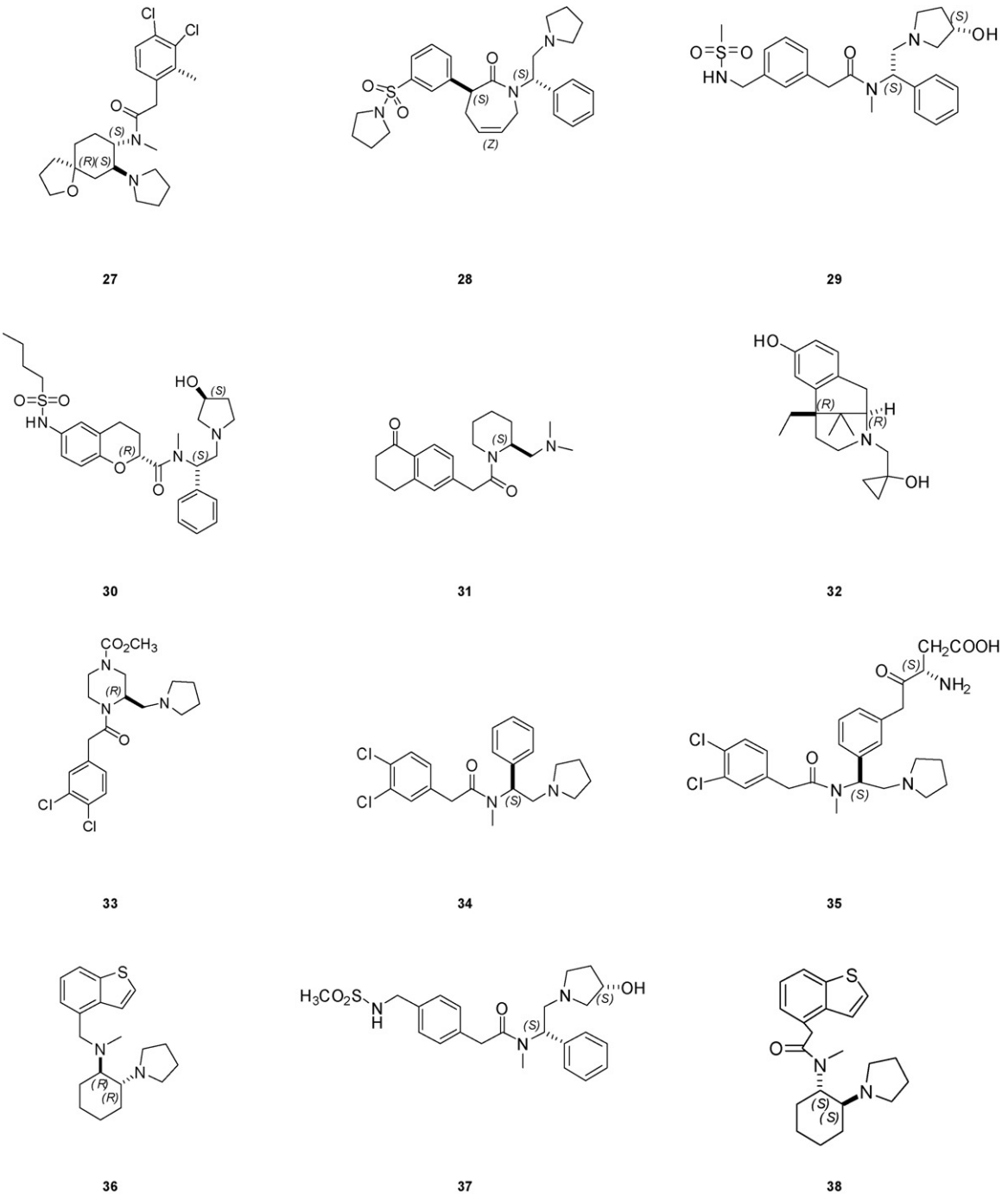

Fig. 2. Chemical structures of compounds in test set. All structures were drawn using *ChemDraw Ultra* 8.0.

features, and the removal or addition of features from the models. Each perturbation is evaluated by consideration of three cost components, the error, the configuration, and the weight cost. By default, the 10 lowest cost hypotheses are written to the output file.

Each feature of a hypothesis represents a certain order of magnitude of the compounds' activity. With the default setting of 0.302, the represented orders of magnitude are kept as close to 2 as possible. The weight component is a value that increases in a Gaussian form as this feature weight in a model deviates from the idealized value of 2. The configuration cost (also known as entropy cost) penalizes the complexity of the pharmacophore hypothesis space while the error cost penalizes the deviation between the estimated activities of the training set and experimentally determined values. The two additional theoretical cost calculations are the fixed cost and the null cost. The fixed cost represents the simplest model that fits all the data perfectly and is calculated by the minimum achievable error and weight cost and the constant configuration cost. The null cost represents the maximum cost of a pharmacophore with no features and estimates activity data of every molecule in the training set as the average of all activities in the set. Therefore, the contribution from the weight or configuration component does not apply. Its absolute value is equal to the maximum occurring error cost [40].

3. Quality assessment of the pharmacophore hypotheses

3.1. Cost function analysis

The quality of the generated hypotheses was evaluated by considering the cost functions (represented in bits unit) relative to the null and the fixed hypothesis calculated by the *Catalyst*/HypoGen module during the hypothesis generation. The total cost of any hypothesis should be toward the value of the fixed cost to represent any useful model. It has been suggested in the *Catalyst* software that the differences between the cost of the generated hypothesis and the null hypothesis cost should be as large as possible; a value of 40–60 bits difference may indicate that the hypothesis has a 75–90% chance of representing a true correlation in the data set used. Furthermore, the configuration cost for any generated hypothesis should be less than or equal to 17 (corresponds to 2^{17} pharmacophore models). Any value higher than 17 may indicate that the correlation from any generated pharmacophore is most likely due to chance since *Catalyst* cannot consider more than these models in the optimization phase and so the rest are left out of the process. The error cost should also be low; this value increases as the value of the rms increases. The rmsd represents the quality of the correlation between the estimated and the actual activity data.

3.2. Cross-validation test

To further assess the statistical significance of the pharmacophore hypotheses generated from the training set molecules, a validation procedure based on Fischer's randomization test was applied [41]. The point of this test is to establish the strong correlation between chemical structures and biological activity. The activity values of the training set molecules are scrambled randomly using the CatScramble technique, available in the *Catalyst*/HypoGen module, and new spreadsheets are created. The number of spreadsheets generated depends on the level of statistical significance one wants to achieve. For a 95% confidence level, 19 spreadsheets are generated. Similarly, for 98% and 99% confidence levels, 49 and 99 spreadsheets, respectively, are created. In our validation test, 19 spreadsheets were created.

4. Results and discussions

To our knowledge, few systematic studies have been done even though several classes of KOP agonists have been reported. Ronsisvalle and coworkers reported a pharmacophore model considering arylacetamide compounds and benzomorphane derivatives by using the model of the KOP developed by Portoghese and coworkers in 1996 [42,43]. Similar studies have been carried out by Subramanian et al. and Iadanza et al. [44,45]. These authors considered the binding of KOP ligands inside the helix bundle, where the protonated nitrogen of the bound agonist forms a salt bridge to Asp138 carboxylate. Another model of KOP was developed by Wan et al. who included modeling of the three extracellular loops [46]. They reported that dynorphin A may interact with Glu209 of the second extracellular loop, which demonstrates that both binding inside the helix bundle as well as at the extracellular loops are of importance for the binding of the ligands. In 2003, Holzgrabe and Brandt developed a KOP homology model and docked dibenzocyclononanones, ketocyclazocine and arylacetamides in an attempt to understand the pattern of protein–ligand interactions and to explain the high affinity and longer duration of action of dibenzocyclononanones [47]. In 2001 Filizola et al. published a non-specific 3D recognition pharmacophore at the MOP, KOP, and DOP receptors which consisted of a protonated amine, 2 hydrophobic interactions and a centroid of an aromatic ring using 23 non-specific binders selected as potent MOP, KOP, and DOP receptor agonists [48]. However, in this study only five KOP agonists were used to identify the requirements for selective activation by distance analysis approach. Additionally for KOP, two HBAs and a hydrophobic moiety was indicated as the determinants for selective activation of KOP with respect to DOP and MOP.

It is of considerable interest to know how structurally different inhibitors are able to induce the same receptor agonistic activity. In general, it is agreed that these compounds may possess the key structural elements that are essential for interacting with the receptor active site. Undoubtedly, a direct docking into the 3D structure of the receptor active site will facilitate new lead molecule discovery. Because the KOP is a membrane-bound GPCR, its X-ray crystal structure is not available. Consequently, the direct structure-based drug design approach is not possible in this case. We assumed that if we could generate a hypothetical pharmacophore definition, as the first essential step toward understanding the interaction between a receptor and a ligand, it will provide a ligand template for a three-dimensional database search and may facilitate lead compound discovery. Subsequently, new drug

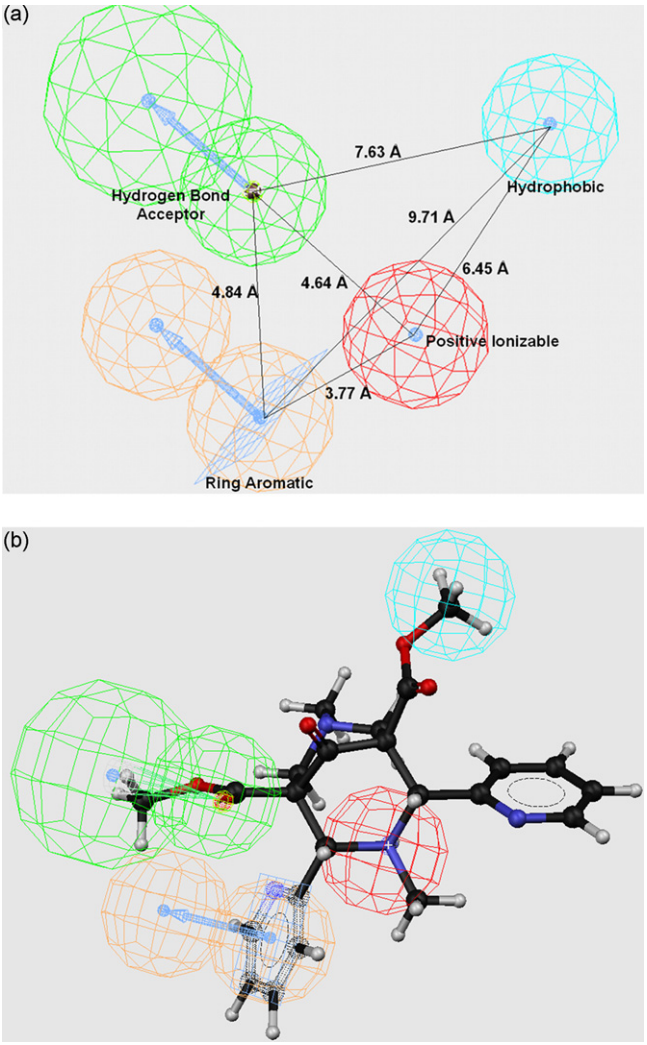

Fig. 3. (a) A representation of the top-ranked hypothesis. (b) Mapping of the most active compound (HZ2; 11) onto the selected pharmacophore hypothesis. The red contour represents the positive ionizable (PI) group while the orange contours represent the ring aromatic (RA) features. The green and blue contours represent hydrogen bond acceptors (HBA) and hydrophobic (HYD) features, respectively.

Table 1
Results obtained from pharmacophore hypothesis generation using the training set molecules[a]

Hypo number.	Total cost	Configuration cost	rms	Correlation	Features[b]
1	127.45	15.53	1.21	0.87	HBA, HYD, PI, RA
2	129.47	15.52	1.31	0.84	HBA, HYD, PI, RA
3	133.58	15.52	1.43	0.81	HBA, HYD, PI, RA
4	134.97	15.52	1.42	0.82	HBA, HYD, PI, RA
5	135.71	15.52	1.56	0.76	HBA, HBA, HYD, HYD
6	135.78	15.52	1.54	0.77	HBA, HYD, HYD, PI
7	136.03	15.53	1.51	0.78	HBA, HYD, PI, RA
8	137.07	15.53	1.57	0.76	HBA, HYD, PI, RA
9	138.01	15.53	1.51	0.79	HBA, HYD, HYD, RA
10	139.31	15.53	1.64	0.73	HBA, HBA, HYD, HYD

[a] Null cost = 162.70. Fixed cost = 104.11. Configuration cost = 15.53. All costs are in units of bits.
[b] HBA, hydrogen bond acceptor; HYD, hydrophobic; PI, positive ionizable; RA, ring aromatic.

candidates may be obtained via the optimization of new leads found using the pharmacophore model.

4.1. Pharmacophore generation

A set of 10 pharmacophore hypotheses was generated using 26 training set compounds listed in Fig. 1. The results of the hypotheses, which include different cost values calculated during the generation of hypotheses along with rmsd, correlation, and pharmacophoric features, have been listed in Table 1. The total cost value of each hypothesis was close to the fixed cost values, which is expected for a good hypothesis. The entropy (configuration cost) values of the hypotheses were also within the allowed range. The difference between the null hypothesis and the fixed cost and the total cost of the best hypothesis were 58.59 bits and 35.25 bits, respectively, which are close to the recommended values for a valid hypothesis. Since hypothesis 1 had the best values in terms of total cost, error cost, rms differences, and the highest correlation, it was selected for further use (Fig. 3a). Table 2 shows the actual and estimated K_i values of the training set compounds calculated on the basis of hypothesis 1. It is notable that only one moderately active (++) compound was estimated to be inactive (−).

4.2. Pharmacophore assessment

The quality of the pharmacophore was assessed using the CatScramble technique in *Catalyst*. The purpose of using this technique is to generate pharmacophore hypotheses using the same features and parameters used to develop the original pharmacophore hypothesis but with randomized activity data among the training set compounds. If the randomized sets generate pharmacophores with similar or better cost values, rms, and correlation, then the original pharmacophore can be considered to have been generated by chance. The results obtained from the CatScramble runs indicated that hypotheses generated after randomization had no predictive value. This cross-validation technique provided confidence for the pharmacophore generated from the training set molecules.

The selected pharmacophore was further validated by two techniques: (a) by assessing the predictive ability of the pharmacophore on test set molecules; (b) and by incorporating an external set of negative controls consisting of five marketed drugs acting on central nervous systems, which target different G-protein coupled receptors. Additionally, salvinorin A and 6-GNTI were included as negative controls. Though both compounds are KOP agonists, they are thought to interact at a different binding site [49,50]. In *Catalyst*, it is assumed that all of the compounds used for pharmacophore model generation bind to the same active site in the same way. A molecule that either misses an important feature or the feature is present but cannot be oriented correctly in space will be predicted as inactive. Consequently, if valid, the generated pharmacophore will not predict these agents as highly active (represented as +++).

Table 2
Actual and estimated activities of training set molecules calculated on the basis of the top-ranked hypothesis

Name	Actual K_i (nM)	Estimated K_i (nM)	Activity scale[a]	Estimated activity scale	Reference
1	0.058	0.16	+++	+++	[17]
2	1.6	3.2	++	++	[19]
3	1900	1500	–	–	[22]
4	8.7	4.6	++	++	[20]
5	99	6.2	++	++	[19]
6	0.31	0.79	+++	+++	[21]
7	0.11	0.14	+++	+++	[23,24]
8	16	39	++	++	[16]
9	2300	1800	–	–	[17]
10	1.2	0.89	++	+++	[15]
11	0.015	9.9e-03	+++	+++	[26]
12	4.2	11	++	++	[25]
13	0.78	2	+++	++	[27]
14	0.69	1.4	+++	++	[24]
15	0.87	0.92	+++	+++	[16,26]
16	0.69	1.2	+++	++	[24,29]
17	0.2	0.79	+++	+++	[30]
18	2.7	0.56	++	+++	[17]
19	0.63	1.2	+++	++	[17]
20	0.34	0.25	+++	+++	[22]
21	0.41	1.1	+++	++	[21]
22	0.57	2.1	+++	++	[28]
23	0.36	0.16	+++	+++	[17]
24	0.5	1	+++	+++	[27]
25	180	4.6	+	++	[32]
26	0.62	0.49	+++	+++	[30]

[a] Highly active ($\leq$1 nM, +++), moderately active (1 $<$ 100 nM, ++), active (100 $\leq$ 500 nM, +) and inactive ($>$500 nM, −).

Table 3
Actual and estimated activities of test set molecules calculated on the basis of the top-ranked hypothesis

Name	Actual K_i (nM)	Estimated K_i (nM)	Activity scale[a]	Estimated activity scale	Reference
27	7.6	1.4	++	++	[34]
28	0.31	1	+++	+++	[33]
29	10	1.9	++	++	[20]
30	1.6	2.4	++	++	[19]
31	47	1.2	++	++	[28]
32	0.12	30	+++	++	[24,33]
33	0.45	0.8	+++	+++	[33]
34	0.43	0.94	+++	+++	[22]
35	0.34	0.47	+++	+++	[15]
36	8100	510	–	–	[31]
37	0.6	2.3	+++	++	[20]
38	3.7	4.3	++	++	[25]

[a] Highly active (≤1 nM, +++), moderately active (1 < 100 nM, ++), active (100 ≤ 500 nM, +), and inactive (>500 nM, –).

4.3. Validation of pharmacophores

4.3.1. Validation of pharmacophore using test set compounds

The validity of any pharmacophore model needs to be determined by applying that model to the test set to find out how correctly the model predicts the activity of the test set molecules and, more importantly, whether it can correctly identify active and inactive molecules. The selected pharmacophore was validated with a test set containing 12 compounds obtained from the same laboratories as that of the training set compounds. This validation gives additional confidence in the utility of the selected pharmacophore. The estimated activities were scored using

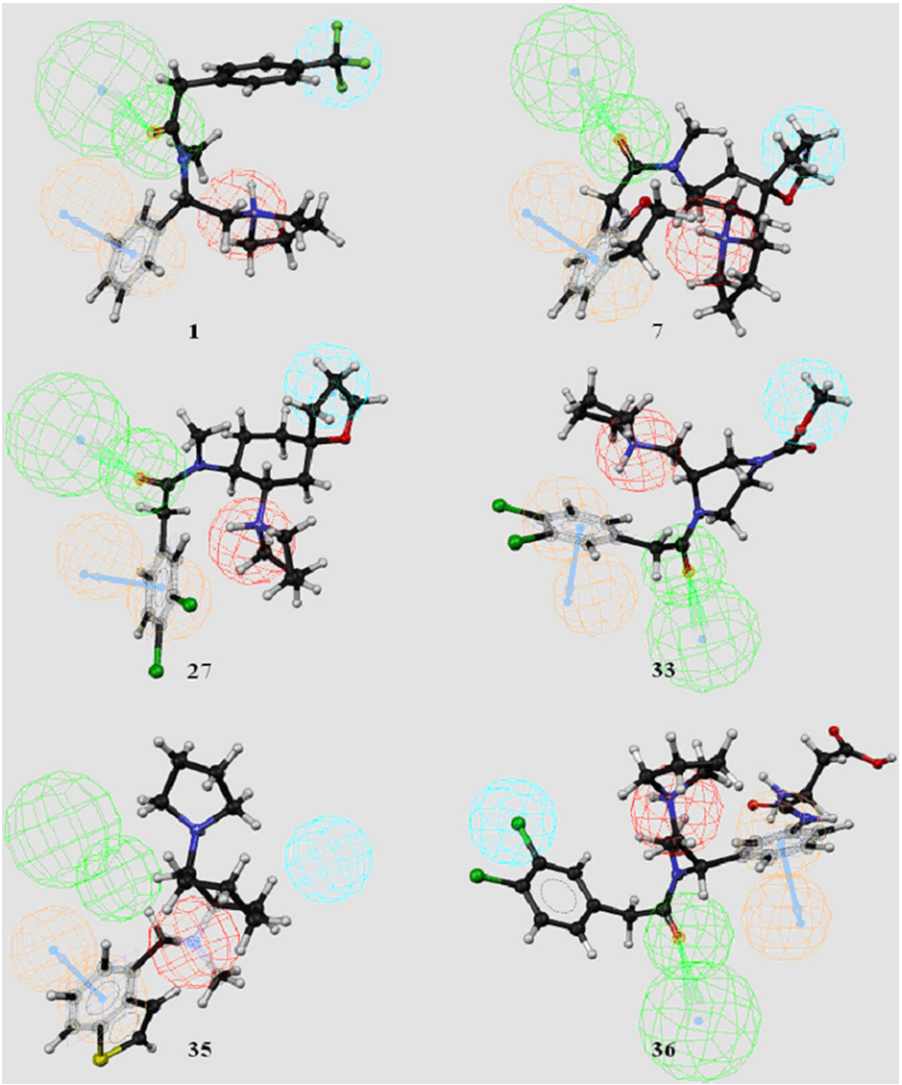

Fig. 4. Mapping of different compounds from both training and test set onto the selected pharmacophore. The red contour represents the PI group while the orange contours represent the RA features. The green and blue contours represent HBA and HYD features, respectively.

hypothesis 1 and reported in Table 3. Out of 12 compounds, 10 were accurately predicted. Only two highly active compounds were classified as moderately active. The selected pharmacophore clearly showed minimal failure in classifying compounds correctly. The most potent compound in the training set, HZ2 (compound 11 in Fig. 1 and Table 2) was chosen to show mapping onto the selected hypothesis (Fig. 3b). In addition, mapping of two highly active compounds from the training set and two highly active, one moderately active and one inactive from the test set are also shown in Fig. 4. The "best fit" option was selected in all cases.

4.3.2. Validation with negative controls

None of the negative controls could be mapped onto the selected pharmacophore (see supporting information; Table S1) and all were estimated to be inactive, thus confirming the validity of the model in a negative test.

This validation further confirmed the effectiveness of the derived pharmacophore model, which will likely be useful in identifying NCEs that target KOP. Additionally, this pharmacophore may also be used in de novo design to develop novel drugs that satisfy the pharmacophoric requirements. Furthermore, it can guide the synthesis of new analogues during lead optimization.

5. Conclusions

A pharmacophore model, developed from a novel automated training set selection protocol, was generated for classical KOP agonists. The model consists of four features: a hydrogen bond acceptor, a hydrophobic interaction, a ring aromatic, and a positive ionizable moiety. This pharmacophore model was shown to identify chemical functional features that were characteristic of active compounds, accurately differentiating the actives from the inactives. The pharmacophores' reliability in quantitative terms was verified in several validation procedures. To our knowledge this is the first attempt to account for several structurally unrelated KOP agonists belonging to different activity classes. In consideration of the enormous effort of in vitro screening of large compound libraries, the generated pharmacophore may serve as a fast and powerful tool for *in silico* database mining. Efforts are ongoing in our laboratory to identify novel molecular scaffolds that could serve as leads for synthetic modification in order to restrict access into the CNS. We believe that such an approach could significantly reduce the cost of uncovering new leads within the drug discovery and development process.

Acknowledgments

This work was supported by NIH grant P20 RR 021929-01. NS is grateful to Prof. Rae Matsumoto for the award of Center of Research Excellence in Natural Products Neuroscience (CORE-NPN) fellowship.

Appendix A. Supplementary data

Supplementary data associated with this article can be found, in the online version, at doi:10.1016/j.jmgm.2008.03.007.

References

[1] M. Minami, M. Satoh, Molecular biology of the opioid receptors: structures, functions and distributions, Neurosci. Res. 23 (1995) 121–145.
[2] M. Satoh, M. Minami, Molecular pharmacology of the opioid receptors, Pharmacol. Ther. 68 (1995) 343–364.
[3] M.J. Millan, Multiple opioid systems and pain, Pain 27 (1986) 303–347.
[4] W.R. Martin, Pharmacology of opioids, Pharmacol. Rev. 35 (1983) 283–323.
[5] W.R. Martin, C.G. Eades, J.A. Thompson, R.E. Huppler, P.E. Gilbert, The effects of morphine- and nalorphine-like drugs in the nondependent and morphine-dependent chronic spinal dog, J. Pharmacol. Exp. Ther. 197 (1976) 517–532.
[6] A. Pande, R.E. Pyke, M. Greiner, S.A. Cooper, R. Benjamin, M.W. Peirce, Analgesic efficacy of the κ-receptor agonist, enadoline, in dental surgery pain, Clin. Neuropharmacol. 19 (1996) 92–97.
[7] A. Pande, R.E. Pyke, M. Greiner, G.L. Wideman, R. Benjamin, M.W. Pierce, Analgesic efficacy of enadoline versus placebo or morphine in postsurgical pain, Clin. Neuropharmacol. 19 (1996) 451–456.
[8] V. Kumar, M.A. Marella, L. Cortes-Burgos, et al., Arylacetamides as peripherally restricted kappa opioid receptor agonists, Bioorg. Med. Chem. Lett. 10 (2000) 2567–2570.
[9] Q. Zhang, M. Schaffer, R. Elde, C. Stein, Effects of neurotoxins and hindpaw inflammation on opioid receptor immunoreactivities in dorsal root ganglia, Neuroscience 85 (1998) 281–291.
[10] P.J. Riviere, Peripheral kappa-opioid agonists for visceral pain, Br. J. Pharmacol. 141 (2004) 1331–1334.
[11] J. Shaw, J.A. Carroll, P. Alcock, B.G. Main, ICI 204448: a kappa-opioid agonist with limited access to the CNS, Br. J. Pharmacol. 96 (1989) 986–992.
[12] A. Bickel, S. Dorfs, M. Schmelz, C. Forster, W. Uhl, H.O. Handwerker, Effects of antihyperalgesic drugs on experimentally induced hyperalgesia in man, Pain 76 (1998) 317–325.
[13] H. Kramer, W. Uhl, B. Ladstetter, A. Backer, Influence of asimadoline, a new κ-opioid receptor agonist, on tubular water absorption and vasopressin secretion in man, Br. J. Pharmacol. 50 (2000) 227–235.
[14] H. Machelska, M. Pfluger, W. Weber, et al., Peripheral effects of the κ-opioid agonist EMD 61753 on pain and inflammation in rats and humans, J. Pharmacol. Exp. Ther. 290 (1999) 354–361.
[15] A.C. Chang, A. Cowan, A.E. Takemori, P.S. Portoghese, Aspartic acid conjugates of 2-(3,4-dichlorophenyl)-*N*-methyl-*N*-[(1*S*)-1(3-aminophenyl)-2-(1-pyrrolidinyl) ethyl]acetamide: kappa opioid receptor agonists with limited access to the central nervous system, J. Med. Chem. 39 (1996) 4478–4482.
[16] D.L. DeHaven-Hudkins, R.E. Dolle, Peripherally restricted opioid agonists as novel analgesic agents, Curr. Pharm. Des. 10 (2004) 743–757.
[17] V. Kumar, D. Guo, J.A. Cassel, et al., Synthesis and evaluation of novel peripherally restricted kappa-opioid receptor agonists, Bioorg. Med. Chem. Lett. 15 (2005) 1091–1095.
[18] Catalyst, version 4.8, Burlington, Accelrys Inc., 2003.
[19] G.H. Chu, M. Gu, J.A. Cassel, et al., Potent and highly selective kappa opioid receptor agonists incorporating chroman- and 2,3-dihydrobenzofuran-based constraints, Bioorg. Med. Chem. Lett. 15 (2005) 5114–5119.
[20] B. Le Bourdonnec, C.W. Ajello, P.R. Seida, et al., Arylacetamide kappa opioid receptor agonists with reduced cytochrome P450 2D6 inhibitory activity, Bioorg. Med. Chem. Lett. 15 (2005) 2647–2652.
[21] G. Ronsisvalle, O. Prezzavento, L. Pasquinucci, et al., CCB, a novel specific kappa opioid agonist, which discriminates between opioid and sigma 1 recognition sites, Life Sci. 57 (1995) 1487–1495.
[22] P.A. Tuthill, P.R. Seida, W. Barker, et al., Azepinone as a conformational constraint in the design of kappa-opioid receptor agonists, Bioorg. Med. Chem. Lett. 14 (2004) 5693–5697.
[23] S.L. Walsh, E.C. Strain, M.E. Abreu, G.E. Bigelow, Enadoline, a selective kappa opioid agonist: comparison with butorphanol and hydromorphone in humans, Psychopharmacology (Berl.) 160 (2001) 170–181.
[24] J.C. Hunter, G.E. Leighton, K.G. Meecham, et al., CI-977, a novel and selective agonist for the kappa-opioid receptor, Br. J. Pharmacol. 101 (1990) 183–189.
[25] C.R. Clark, P.R. Halfpenny, R.G. Hill, et al., Highly selective kappa opioid analgesics. Synthesis and structure-activity relationships of novel *N*-[2-aminocyclohexylaryl]acetamide and *N*-[2-aminocyclohexylaryloxy]acetamide derivatives, J. Med. Chem. 31 (1988) 831–836.
[26] T. Siener, A. Cambareri, U. Kuhl, et al., Synthesis and opioid receptor affinity of a series of 2, 4-diaryl-substituted 3,7-diazabicylononanones, J. Med. Chem. 43 (2000) 3746–3751.
[27] A. Cappelli, M. Anzini, S. Vomero, et al., Synthesis, biological evaluation, and quantitative receptor docking simulations of 2-[(acylamino)ethyl]-1,4-benzodiazepines as novel tifluadom-like ligands with high affinity and selectivity for kappa-opioid receptors, J. Med. Chem. 39 (1996) 860–872.
[28] G. Giardina, G.D. Clarke, G. Dondio, G. Petrone, M. Sbacchi, V. Vecchietti, Selective kappa-opioid agonists: synthesis and structure-activity relationships of piperidines incorporating on oxo-containing acyl group, J. Med. Chem. 37 (1994) 3482–3491.
[29] G. Ronsisvalle, A. Marrazzo, L. Pasquinucci, O. Prezzavento, M. Pappalardo, F. Vittorio, Specific kappa opioid receptor agonists, Farmaco 56 (2001) 121–125.
[30] V. Vecchietti, G.D. Clarke, R. Colle, G. Giardina, G. Petrone, M. Sbacchi, (1*S*)-1-(Aminomethyl)-2-(arylacetyl)-1,2,3,4-tetrahydroisoquinoline and heterocycle-condensed tetrahydropyridine derivatives: members of a novel class of very potent kappa opioid analgesics, J. Med. Chem. 34 (1991) 2624–2633.
[31] P.R. Halfpenny, R.G. Hill, D.C. Horwell, et al., Highly selective kappa-opioid analgesics. Part 2. Synthesis and structure–activity relationships of novel *N*-[(2-aminocyclohexyl)aryl]acetamide derivatives, J. Med. Chem. 32 (1989) 1620–1626.
[32] V. Kumar, D. Guo, J.D. Daubert, et al., Amino acid conjugates as kappa opioid receptor agonists, Bioorg. Med. Chem. Lett. 15 (2005) 1279–1282.
[33] S. Soukara, C.A. Maier, U. Predoiu, A. Ehret, R. Jackisch, B. Wunsch, Methylated analogues of methyl (R)-4-(3,4-dichlorophenylacetyl)-3-(pyrrolidin-1-ylmethyl)piperazine-1-carboxylate (GR-89,696) as highly potent kappa-receptor

agonists: stereoselective synthesis, opioid-receptor affinity, receptor selectivity, and functional studies, J. Med. Chem. 44 (2001) 2814–2826.
[34] J. Szmuszkovicz, P.F. Von Voigtlander, Benzeneacetamide amines: structurally novel non-mu opioids, J. Med. Chem. 25 (1982) 1125–1126.
[35] O. Guner, O. Clement, Y. Kurogi, Pharmacophore modeling and three dimensional database searching for drug design using Catalyst: recent advances, Curr. Med. Chem. 11 (2004) 2991–3005.
[36] P. Gund, Progress in Molecular and Subcellular Biology, Springer-Verlag, New York, 1977.
[37] B.R. Brooks, R.E. Bruccoleri, B.D. Olafson, D.J. States, S. Swaminathan, M. Karplus, CHARMM: a program for macromolecular energy, minimization, and dynamics calculations, J. Comput. Chem. 4 (1983) 187–217.
[38] A. Smellie, S.L. Teig, P. Towbin, Poling: promoting conformational variation, J. Comput. Chem. 16 (1995) 171–187.
[39] English Philosopher and Franciscan Monk, William of Ockham, p. 1285.
[40] J. Sutter, O.F. Guner, R. Hoffman, H. Li, M. Waldman, Pharmacophore: Perception, Development and Use in Drug Design, International University Line, La Jolla, 1999
[41] R. Fischer, The Design of Experiments, 8th ed., Hafner Publishing Co., New York, 1966.
[42] A. Lavecchia, G. Greco, E. Novellino, F. Vittorio, G. Ronsisvalle, Modeling of kappa-opioid receptor/agonists interactions using pharmacophore-based and docking simulations, J. Med. Chem. 43 (2000) 2124–2134.
[43] T.G. Metzger, M.G. Paterlini, P.S. Portoghese, D.M. Ferguson, Application of the message-address concept to the docking of naltrexone and selective naltrexone-derived opioid antagonists into opioid receptor models, Neurochem. Res. 21 (1996) 1287–1294.
[44] M. Iadanza, M. Holtje, G. Ronsisvalle, H.D. Holtje, Kappa-opioid receptor model in a phospholipid bilayer: molecular dynamics simulation, J. Med. Chem. 45 (2002) 4838–4846.
[45] G. Subramanian, M.G. Paterlini, D.L. Larson, P.S. Portoghese, D.M. Ferguson, Conformational analysis and automated receptor docking of selective arylacetamide-based kappa-opioid agonists, J. Med. Chem. 41 (1998) 4777–4789.
[46] X.H. Wan, X.Q. Huang, D.H. Zhou, H.L. Jiang, K.X. Chen, Z.Q. Chi, Building 3D-structural model of kappa opioid receptor and studying its interaction mechanism with dynorphin A(1-8), Acta Pharmacol. Sin. 21 (2000) 701–708.
[47] U. Holzgrabe, W. Brandt, Mechanism of action of the diazabicyclononanone-type kappa-agonists, J. Med. Chem. 46 (2003) 1383–1389.
[48] M. Filizola, H.O. Villar, G.H. Loew, Differentiation of delta, mu, and kappa opioid receptor agonists based on pharmacophore development and computed physicochemical properties, J. Comput. Mol. Des. 15 (2001) 297–307.
[49] N. Singh, G. Chevé, D.M. Ferguson, C.R. McCurdy, A combined ligand-based and target-based drug design approach for G-protein coupled receptors: application to salvinorin A, a selective kappa opioid receptor agonist, J. Comput. Mol. Des. 20 (2006) 471–493.
[50] B. Kane, M. Nieto, C. McCurdy, D. Ferguson, A unique binding epitope for salvinorin A, a non-nitrogenous kappa opioid receptor agonist, FEBS J. 273 (2006) 1966–1974.